

# Point Pattern Matching with Robust Spectral Correspondence

Marco Carcassoni and Edwin R. Hancock  
Department of Computer Science,  
University of York, York YO1 5DD, UK

## Abstract

*This paper investigates the correspondence matching of point-sets using spectral graph analysis. In particular we are interested in the problem of how the modal analysis of point-sets can be rendered robust to contamination and drop-out. We make three contributions. First, we show how the modal structure of point-sets can be embedded within the framework of the EM algorithm. Second, we present several methods for computing the probabilities of point correspondences using the point proximity matrix. Third, we consider alternatives to the Gaussian proximity matrix. We evaluate the new method on both synthetic and real-world data. Here we show that the method can be used to compute useful correspondences even when the level of point contamination is as large as 50%.*

## 1 Introduction

Spectral graph theory is a term applied to a family of techniques that aim to characterise the global structural properties of graphs using the eigenvalues and eigenvectors of the adjacency matrix [1]. Although the subject has found widespread use in a number of areas including structural chemistry and routeing theory, there have been relatively few applications in the computer vision literature. The reason for this is that although elegant, spectral graph representations are notoriously susceptible to the effect of structural error. In other words, spectral graph theory can furnish very efficient methods for characterising exact relational structures, but soon breaks down when there are spurious nodes and edges in the graphs under study.

Spectral methods for graph analysis invariably commence by computing the Laplacian matrix. This is closely related to the node adjacency matrix. The diagonal elements of the Laplacian matrix are equal to the degree of the nodes (vertices) and the off diagonal elements are unity if the corresponding nodes are connected by an edge, and are zero otherwise. However, it is also common to work with proximity or property matrices where the off diagonal elements reflect the difference in node attributes such as position [8] or orientation [7]. Once a matrix characterisation of the graph is to hand then the eigenvalues and eigenvectors are computed. The main idea behind spectral graph theory is

to use the distribution of eigenvalues to provide a compact summary of graph-structure.

In the computer vision literature there have been a number of attempts to use spectral properties for graph-matching, object recognition and image segmentation. Umeyama has an eigendecomposition method that matches graphs of the same size [12]. Borrowing ideas from structural chemistry, Scott and Longuet-Higgins were among the first to use spectral methods for correspondence analysis [6]. They showed how to recover correspondences via singular value decomposition on the point association matrix between different images. In keeping more closely with the spirit of spectral graph theory, yet seemingly unaware of the related literature, Shapiro and Brady [8] developed an extension of the Scott and Longuet-Higgins method, in which point sets are matched by comparing the eigenvectors of the point proximity matrix. Here the proximity matrix is constructed by computing the Gaussian weighted distance between points. The eigen-vectors of the proximity matrices can be viewed as the basis vectors of an orthogonal transformation on the original point identities. In other words, the components of the eigenvectors represent mixing angles for the transformed points. Matching between different point-sets is effected by comparing the pattern of eigenvectors in different images. Shapiro and Brady's method can be viewed as operating in the attribute domain rather than the structural domain. Horaud and Sossa have adopted a purely structural approach to the recognition of line-drawings. Their representation is based on the immanantal polynomials for the Laplacian matrix of the line-connectivity graph. By comparing the coefficients of the polynomials, they are able to index into a large data-base of line-drawings. In another application involving indexing into large data-bases, Sengupta and Boyer have used property matrix spectra to characterise line-patterns. Various attribute representations are suggested and compared. Shokoufandeh, Dickinson and Siddiqi [10] have shown how graphs can be encoded using local topological spectra for shape recognition from large data-bases. Finally, a number of authors have used spectral methods to perform pairwise clustering on image data. Shi and Malik [9] use the second eigenvalue to segment images by performing an eigen-

decomposition on a matrix of pairwise attribute differences. Inoue and Urahama [4] have shown how the sequential extraction of eigen-modes can be used to cluster pairwise pixel data.

The focus of this paper is the use of property matrix spectra for correspondence matching. As mentioned above, spectral methods offer an attractive route to correspondence matching since they provide a representation that can be used to characterise graph structure at the global level. If used effectively, the spectral representation can be used for rapid matching by comparing patterns of eigenvalues or eigenvectors. Conventional graph-matching methods, on the other hand, rely on local structural decompositions. Correspondence analysis is achieved through the iterative propagation of local consistency constraints with the hope of achieving global consistency. Moreover, accuracy is traded against the efficiency gains achieved by using increasingly localised structures. Invariably, global consistency is only assessed using the edges of the graphs. However, the increased fidelity of representation achieved using a global spectral representation must be weighed against their relative fragility to the addition of noise and clutter. For instance, although the methods of Horaud and Sossa [11] and of Shapiro and Brady [8] work well for graphs that are free of structural contamination, they do not work well when the graphs are of different size. Moreover, the method of Sengupta and Boyer [7], although relatively robust is not concerned with detailed correspondence analysis.

Our aim in this paper is to consider how spectral methods can be rendered robust for correspondence matching with point-sets which contain significant noise and contamination. To do this we make three contributions. First we cast the problem of correspondence matching in the framework of the EM algorithm. This gives us scope for outlier reject via weighting in the expectation step. The framework used as the starting point for our study is the dual-step EM algorithm of Cross and Hancock [2]. This work has shown how local relational constraints can be embedded in an EM algorithm for point alignment under affine and perspective distortion. We commence by showing how graph-spectra can be used to compute the required correspondence probabilities in a manner which is both efficient and global. Our second contribution is to consider how to make the initial computation of the point proximity matrix more robust to contamination by the addition of clutter and the relative movement of points due to measurement noise. Finally, we consider how to compare the node mixing angles in a robust manner.

## 2 Prerequisites

The aim in this paper is to use the dual-step EM algorithm of Cross and Hancock [2] to render the process of

spectral pattern matching robust. Before we detail the algorithm, we provide some of the formal ingredients of the method.

### 2.1 Affine Geometry

Suppose that  $\Phi^{(n)}$  is the geometric transformation that best aligns a set of image feature points  $\mathbf{w}$  with their counterparts in a model. Each point in the image data set is represented by an augmented position vector  $\vec{w}_i = (x_i, y_i, 1)^T$  where  $i$  is the point index. This augmented vector represents the two-dimensional point position in a homogeneous coordinate system. We will assume that all these points lie on a single plane in the image. In the interests of brevity we will denote the entire set of image points by  $\mathbf{w} = \{\vec{w}_i, \forall i \in \mathcal{D}\}$  where  $\mathcal{D}$  is the point set. The corresponding fiducial points constituting the model are similarly represented by  $\mathbf{z} = \{\vec{z}_j, \forall j \in \mathcal{M}\}$  where  $\mathcal{M}$  denotes the index-set for the model feature-points  $\vec{z}_j$ .

In this paper we confine our attention to affine transformations. The affine transformation has six free parameters. These model the two components of translation of the origin on the image plane, the overall rotation of the co-ordinate system, the overall scale together with the two parameters of shear. These parameters can be combined succinctly into an augmented matrix that takes the form

$$\Phi^{(n)} = \begin{pmatrix} \phi_{1,1}^{(n)} & \phi_{1,2}^{(n)} & \phi_{1,3}^{(n)} \\ \phi_{2,1}^{(n)} & \phi_{2,2}^{(n)} & \phi_{2,3}^{(n)} \\ 0 & 0 & 1 \end{pmatrix} \quad (1)$$

With this representation, the affine transformation of co-ordinates is computed using the matrix multiplication  $\vec{w}_i^{(n)} = \Phi^{(n)} \vec{w}_i$ . Clearly, the result of this multiplication gives us a vector of the form  $\vec{w}_i^{(n)} = (x, y, 1)^T$ . The superscript  $n$  indicates that the parameters are taken from the  $n^{th}$  iteration of our algorithm.

### 2.2 Correspondences

The recovery of the parameters of the transformation matrix  $\Phi^{(n)}$ , requires correspondences between the point-sets. In other words, we need to know which point in the data aligns with which point in the model. This set of correspondences between the two point sets is denoted by the function  $f^{(n)} : \mathcal{M} \rightarrow \mathcal{D}$  from the nodes of the data-graph to those of the model graph. According to this notation the statement  $f^{(n)}(i) = j$  indicates that there is a match between the node  $i \in \mathcal{D}$  of the model-graph to the node  $j \in \mathcal{M}$  of the data-graph at iteration  $n$  of the algorithm.

## 3 The Dual-step EM Algorithm

Cross and Hancock's contribution was to present an extension of the standard EM algorithm in which the structural consistency of correspondences matches can be used

to gate contributions to the expected log-likelihood function [2]. This idea is closely related to the hierarchical mixture of experts algorithm of Jordan and Jacobs [5]. However, the method uses a dictionary method for computing the correspondence probabilities which is both localised and time consuming. The aim here is to replace the dictionary-based method used to compute the probabilities with a robust spectral method.

### 3.1 Expected Log-likelihood

According to Cross and Hancock we seek both correspondence matches (i.e. the function  $f$ ) and transformation parameters which maximise the expected log-likelihood

$$Q(\Phi^{(n+1)}|\Phi^{(n)}) = \sum_{(i,j) \in \mathcal{D} \times \mathcal{M}} P(\tilde{z}_j|\vec{w}_i, \Phi^{(n)}) \zeta_{i,j}^{(n)} \ln p(\vec{w}_i|\tilde{z}_j, \Phi^{(n)}). \quad (2)$$

The meaning of this expected log-likelihood function requires further comment. The measurement densities  $p(\vec{w}_i|\tilde{z}_j, \Phi^{(n+1)})$  model the distribution of error-residuals between the data-point position  $\vec{w}_i$  and the model point position  $\tilde{z}_j$  at iteration  $n$  of the algorithm. The log-likelihood contributions at iteration  $n+1$  are weighted by the *a posteriori* measurement probabilities  $P(\tilde{z}_j|\vec{w}_i, \Phi^{(n)})$  computed at the previous iteration  $n$  of the algorithm. The individual contributions to the expected log-likelihood function are gated by the structural matching probabilities  $\zeta_{i,j}^{(n)}$ . These probabilities measure the consistency of the pattern of correspondences when the match  $f^{(n)}(i) = j$  is made. Their modelling is the topic of Section 4.

### 3.2 Expectation

In the expectation step of the EM algorithm the *a posteriori* probabilities of the missing data (i.e. the model-graph measurement vectors,  $\tilde{z}_j$ ) are updated by substituting the point positions vector into the conditional measurement distribution. Using the Bayes rule, we can re-write the *a posteriori* measurement probabilities in terms of the components of the corresponding conditional measurement densities

$$P(\tilde{z}_j|\vec{w}_i, \Phi^{(n)}) = \frac{\alpha_j^{(n)} p(\vec{w}_i|\tilde{z}_j, \Phi^{(n)})}{\sum_{j' \in \mathcal{M}} \alpha_{j'}^{(n)} p(\vec{w}_i|\tilde{z}_{j'}, \Phi^{(n)})}. \quad (3)$$

The mixing proportions are computed by averaging the *a posteriori* probabilities over the set of data-points, i.e.  $\alpha_j^{(n+1)} = \frac{1}{|\mathcal{D}|} \sum_{i \in \mathcal{D}} P(\tilde{z}_j|\vec{w}_i, \Phi^{(n)})$ . In order to proceed with the development of a point registration process we require a model for the conditional measurement densities, i.e.  $p(\vec{w}_i|\tilde{z}_j, \Phi^{(n)})$ . Here we assume that the required model can be specified in terms of a multivariate Gaussian distribution. The random variables appearing in these distributions are the error residuals for the position predictions of the  $j$ th

model point delivered by the current estimated data-point positions. Accordingly we write

$$p(\vec{w}_i|\tilde{z}_j, \Phi^{(n)}) = \frac{1}{2\pi\sqrt{|\Sigma|}} \exp \left[ -\frac{1}{2} \tilde{\epsilon}_{ij}^{(n)\top} \Sigma^{-1} \tilde{\epsilon}_{ij}^{(n)} \right]. \quad (4)$$

In the above expression  $\Sigma$  is the variance-covariance matrix for the position errors and  $\tilde{\epsilon}_{ij}^{(n)} = \tilde{z}_j^{(n)} - \Phi^{(n)} \vec{w}_i$ .

### 3.3 Maximisation

The dual step EM algorithm iterates between the two interleaved maximisation steps for alignment parameter estimation and estimating correspondence assignments.

Point correspondences are sought so as to maximise the *a posteriori* probability of structural match. The update formula is

$$f^{(n+1)}(i) = \arg \max_{j \in \mathcal{M}} P(\tilde{z}_j|\vec{w}_i, \Phi^{(n)}) \zeta_{i,j}^{(n)} \quad (5)$$

In the case of affine geometry, the transformation is linear in the parameters. This allows us to locate the maximum-likelihood parameters directly by solving a system of saddle-point equations for the independent affine parameters. The solution matrix is given by

$$\Phi^{(n+1)} = \left[ \sum_{(i,j) \in f^{(n)}} P(\tilde{z}_j|\vec{w}_i, \Phi^{(n)}) \zeta_{i,j}^{(n)} \vec{w}_i U^T \vec{w}_i^T \Sigma^{-1} \right]^{-1} \times \left[ \sum_{(i,j) \in f^{(n)}} P(\tilde{z}_j|\vec{w}_i, \Phi^{(n)}) \zeta_{i,j}^{(n)} \tilde{z}_j U^T \vec{w}_i^T \Sigma^{-1} \right] \quad (6)$$

where the elements of the matrix  $U$  are the partial derivatives of the affine transformation matrix with respect to the individual parameters.

## 4 Spectral Methods for Correspondence

The aim in this Section is to show how the dual step EM algorithm can be used to render the process of computing correspondences between the nodes of the graphs robust to structural noise and measurement error. The spectral approach to correspondence commences by enumerating a point proximity matrix. This is a continuous counterpart of the graph adjacency matrix. Rather than setting the elements to unity or zero depending on whether or not there is a connecting edge between a pair of nodes, the elements of the proximity matrix are weights that reflect the strength of a pairwise adjacency relation. Once the proximity matrix is to hand, then correspondences are located by computing its eigenvectors. The eigenvectors of the proximity matrix become the columns of a transformation matrix which operates on the original point identities. The rows of the transformation matrix represent the components of the original points in the directions of the eigenvectors. We can locate point correspondences by searching for rows of the transformation matrix which have maximal similarity.

Unfortunately there are two drawbacks with the spectral method of correspondence. Firstly, there is no clear reason

to use Gaussian weighting in favour of possible alternatives. Moreover, the Gaussian weighting may not be the most suitable choice to control the effects of pattern distortion due to point movement under measurement error or deformation under affine or perspective geometry. Secondly, the method proves fragile to structural differences introduced by the addition of clutter or by point drop-out.

The aim in this section is to address these two problems. We commence by considering alternatives to Gaussian weighting. Next we suggest how the comparison of the eigenvectors can be effected in a manner which is robust to measurement error. The contribution is therefore to show how the correspondence probabilities  $\zeta_{i,j}^{(n)}$  can be computed in an efficient and robust manner.

## 4.1 Point Proximity matrix

The role of the weighting function is to model the probability of adjacency relations between points. In Shapiro and Brady's original work the weighting function was the Gaussian [8]. Here we consider various alternative weighting functions suggested by the robust statistics literature.

According to robust statistics, the effects of outliers can be controlled by weighting according to the error-residual. Suppose that  $\Gamma_s(\eta)$  is a weighting function defined on the error-residual  $\eta$ . The parameter  $s$  controls the width of the weighting kernel. Associated with the weighting function is an error-kernel which is defined to be

$$\rho_s(\eta) = \int_{-\infty}^{\eta} \eta' \Gamma_s(\eta') d\eta' \quad (7)$$

There are many choices of possible weighting functions described in the literature. However, they can be classified according to a broad-based taxonomy based on the derivative  $\rho'_s(\eta)$  of the error-kernel. If the derivative is monotonically increasing, then the weighting function is said to be increasing. If the derivative is asymptotically constant, then the weighting function is said to be sigmoidal. Finally, if the derivative asymptotically approaches zero then the weighting function is said to be re-descending.

In this section we investigate several weighting functions which fall into these different classes. Figure 1 shows the graphs of the functions.

### 4.1.1 Gaussian weighted proximity matrix

The standard way to represent the adjacency relations between points is to use the Gaussian proximity matrix. If  $i$  and  $i'$  are two data points, then the corresponding element of the proximity matrix at iteration  $n$  of the algorithm is given by

$$H_D^{(n)}(i, i') = \exp \left[ -\frac{1}{2s^2} \|w_i^{(n)} - w_{i'}^{(n)}\|^2 \right] \quad (8)$$

This weighting function is re-descending.

### 4.1.2 Sigmoidal Proximity Matrix

To provide an example of a sigmoidal weighting function, we consider the proximity matrix generated by the hyperbolic tangent function

$$H_D^{(n)}(i, i') = \frac{2}{\pi \|w_i^{(n)} - w_{i'}^{(n)}\|} \tanh \left[ \frac{\pi}{s} \|w_i^{(n)} - w_{i'}^{(n)}\| \right] \quad (9)$$

### 4.1.3 Increasing Weighting Function

Here we use the increasing weighting function

$$H_D^{(n)}(i, i') = \left[ 1 + \frac{1}{s} \|w_i^{(n)} - w_{i'}^{(n)}\| \right]^{-1} \quad (10)$$

to generate the proximity matrix.

### 4.1.4 Euclidean Weighting Function

Here we investigate the effect of using a weighting function that decreases linearly with distance. We use the following piecewise specification to define a trapezoid function  $H_D^{(n)}(i, i') = T(\|w_i^{(n)} - w_{i'}^{(n)}\|)$  where

$$T(\eta) = \begin{cases} 1 & \text{if } \eta < s_1 \\ 1 - \frac{1}{s_2 - s_1} [\eta - s_1] & \text{if } s_1 < \eta < s_2 \\ 0 & \text{otherwise} \end{cases} \quad (11)$$

Here  $s_1$  is the half-width of the ceiling of the function and  $s_2$  is the half-width of the base.

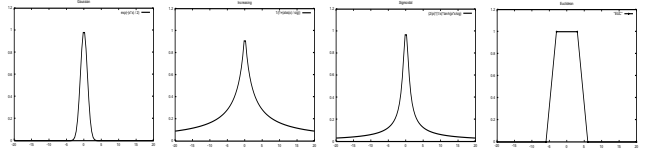


Figure 1. Weighting functions

## 4.2 Correspondences

The modal structure of the two point-sets is found by solving the eigenvalue equation  $HE_l = \lambda_l E_l$ , where  $\lambda_l$  is the  $l^{th}$  eigenvalue of the matrix  $H$  and  $E_l$  is the corresponding eigenvector. We order the vectors according to the size of the associated eigenvalues. The ordered column-vectors are used to construct a modal matrix  $V = (E_1, E_2, E_3, \dots)$ . The column index of this matrix refers to the order of the eigenvalues while the row-index is the index of the original point-set. This modal decomposition is repeated for both the data and the transformed model point-sets to give a data-point modal matrix  $V_D^{(n)}$  and a model-point modal matrix  $V_M$ . Since the two point-sets are potentially of different size, we truncate the modes of the larger point-set. This corresponds to removing the last  $|\mathcal{D}| - |\mathcal{M}|$  rows and columns of the larger matrix. The matrices have  $o = \min[|\mathcal{D}|, |\mathcal{M}|]$  columns.

The modal matrices can be viewed as inducing a linear transformation on the original identities of the point-sets. Each row of the modal matrix represents one of the original points. The column entries in each row measure how the original point identities are distributed among the different eigen-modes.

#### 4.2.1 Shapiro and Brady

Based on this eigendecomposition Shapiro and Brady [8] find correspondences by comparing the rows of the modal matrices  $V_M$  and  $V_D$ . The decision concerning the correspondences is made on the basis of the similarity of different rows in the modal matrices for the data and the model. The measure of similarity is the Euclidean distance between the elements in the corresponding rows. According to Shapiro and Brady the correspondence probabilities are assigned according to the following binary decision

$$\zeta_{i,j} = \begin{cases} 1 & \text{if } j = \arg \min_{j'} \sum_{l=1}^o \|V_D^{(n)}(i, l) - V_M(j', l)\|^2 \\ 0 & \text{otherwise} \end{cases} \quad (12)$$

#### 4.2.2 Correspondence Probabilities

Rather than using the binary correspondence pattern of Shapiro and Brady to gate contributions to the expected log-likelihood function, we can use the elements of the two modal matrices to compute the probabilities of correspondence match. This is done by comparing the elements of the two matrices on a row-by-row basis. A simple way of computing the probabilities is to assume that the vectors are subject to Gaussian measurement errors. As a result, the probability that data-point  $i$  is in correspondence with model data-point  $j$  is equal to

$$\zeta_{i,j}^{(n)} = \frac{\exp \left[ -\mu \sum_{l=1}^o \|V_D^{(n)}(i, l) - V_M(j, l)\|^2 \right]}{\sum_{j' \in \mathcal{M}} \exp \left[ -\mu \sum_{l=1}^o \|V_D^{(n)}(i, l) - V_M(j', l)\|^2 \right]} \quad (13)$$

#### 4.2.3 Robust Correspondence Probabilities

The shortcoming of this method for computing the correspondence probabilities is the effect of outlier measurement errors. When there is a significant difference between one or more of the components of the eigenvectors, then these errors dominate the argument of the exponentials. This will have the tendency to flatten the distribution and will result in ambiguity and equivocation concerning the pattern of correspondences. One way to make the computation of correspondences robust to outlier measurement error is to accumulate probability on a component by component basis over the eigenvectors. To do this we define the correspondence probability to be

$$\zeta_{i,j}^{(n)} = \frac{\sum_{l=1}^o \exp \left[ -\mu \|V_D^{(n)}(i, l) - V_M(j, l)\|^2 \right]}{\sum_{j' \in \mathcal{M}} \sum_{l=1}^o \exp \left[ -\mu \|V_D^{(n)}(i, l) - V_M(j', l)\|^2 \right]} \quad (14)$$

In this way large measurement errors contribute insignificantly through the individual exponentials appearing under the summation over the components of the eigenvectors.

## 5 Experiments

In this section we investigate the performance of the different methods of spectral correspondence reported in this paper. There are three aspects to this experimental study. First we consider the effect of varying the way in which the elements of the point proximity matrix are calculated. Next, we compare the three methods for computing correspondences from the eigenvectors of the proximity matrix. Finally, we show the benefits to be gained from embedding the correspondence process in the EM algorithm.

Our experiments are conducted with random point sets. We investigate two sources of error. The first of these is random measurement error or point-position jitter. Here we subject the positions of the points to Gaussian measurement error. The parameter of the noise process is the standard deviation of the point position error. The second source of error is structural. Here we remove random points. This is the most destructive type of error for spectral methods.

### 5.1 Point Proximity Matrix

Here we investigate the effect of varying the point proximity matrix. The aim is to determine which of the weighting functions returns correspondences which are the most robust to point-position jitter. Figure 2.a shows the fraction of correct correspondences as a function of the standard deviation of the added Gaussian position errors. The standard deviation is recorded as a fraction of the average closest point distance. The best performance is obtained with the increasing weighting function and the trapezoidal Euclidean weighting function. The next best method is the sigmoidal weighting function. The poorest performance is returned by the Gaussian proximity matrix. However, the two best performing weighting functions give a margin of improvement of some 20% over the Gaussian weighting function.

### 5.2 Correspondence Probabilities

In this section we compare the results obtained using different methods for estimating correspondences from the eigenvectors of the point-proximity matrix. In each case we use the increasing weighting function to construct the proximity matrix. We use only the SVD methods to find correspondences. The correspondences are selected on the basis of maximum probability using the different schemes outlined in section 4.2. The effect of embedding the correspondence probabilities in the EM algorithm is deferred until section 5.3.

Figure 2.b shows the fraction of correct correspondences as a function of the standard deviation of the Gaussian measurement error. The results are reported using the ratio of the standard deviation to the average closest inter-point distance. The three curves correspond to the standard method

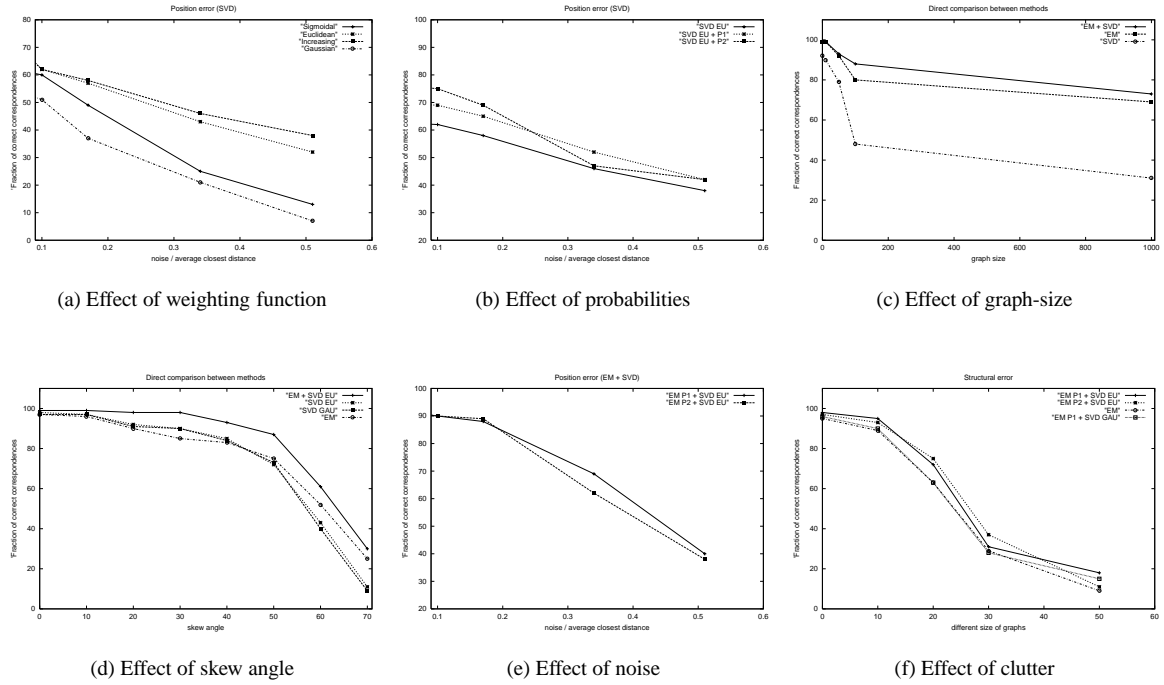


Figure 2. Experimental results

of Shapiro and Brady and the two probabilistic methods outlined in section 4.1. All three methods degrade as the noise standard deviation increases. The two probabilistic methods offer significant improvement over the method of Shapiro and Brady. Although there is little to distinguish the overall performance of the two probabilistic methods, the following pattern emerges: the robust probabilities (section 4.2.3) work best for low noise levels and the simplest probabilistic method (section 4.2.2) gives the best overall performance.

### 5.3 EM Algorithm

In this section we turn our attention to the effect of embedding the correspondence probabilities in the EM algorithm. We compare three different algorithms. The first of these is standard SVD method of Shapiro and Brady. The second is the alignment of the point-sets using the standard EM algorithm. This algorithm does not use any information concerning the pattern of correspondences. Contributions to the log-likelihood function are weighted only by the *a posteriori* alignment probabilities. In other words, we set  $\zeta_{i,j}^{(n)} = 1$  for all values of  $i$  and  $j$ . Finally, we consider the new approach to spectral correspondence developed in this paper. We respectively refer to these algorithms as SVD, EM and EM+SVD.

We commence in Figure 2.c by showing the effect of

positional jitter on the fraction of correct correspondences. The plot shows the fraction of correct matches as a function of the size of the point sets. Here the standard deviation of the Gaussian noise is kept fixed and the size of the point-sets is increased. The two point sets are of the same size. There is no addition or deletion of points. The size of the point-sets is increased by adding new points at random positions. As a result the point-density increases. The main effects to note are the following. Firstly, all three methods degrade with increasing size of the point-sets. One of the reasons for this is that as the size of the point-sets is increased, then so the average inter-point distance decreases. In other words, the degree of relative displacement increases with the increasing number of points. The second feature to note is that the new method (i.e. SVD+EM) consistently gives the best results. Moreover, the performance of the pure SVD method degrades rapidly as the relative displacement of the points is increased. Finally, the SVD+EM method outperforms the EM method by a useful margin.

Next we investigate the effect of controlled affine skew of the point-sets. Figure 2.d shows the fraction of correct correspondences as a function of the skew angle in degrees. Here we compare the standard EM method, the EM method with a trapezoidal weighting function, and the use of pure SVD with a Gaussian weighting function and a trapezoidal weighting function. Here the embedding of the new prox-

imity matrix in the EM algorithm offers clear advantages. There is a 10% margin of improvement for all skew angles.

We now turn to the effect of positional jitter. Figure 2.e compares the effect of using the two different ways of computing the correspondence probabilities. There is no obvious pattern of improvement. However, comparing with Figure 2.b it is clear that the EM method gives a margin of improvement of some 20% over the use of SVD alone.

Finally, we investigate the effects of point-set contamination. Here we add increasing fractions of clutter nodes to the point-sets. We commence by noting that the pure SVD method fails as soon as clutter is added. Hence we can not plot any sensitivity data from the method. Figure 2.f shows the effect of adding controlled fractions of clutter to point-sets of increasing size. The main conclusion to note is that SVD+EM outperforms EM by about 5-10%. Also, as the fraction of clutter increases then so the performance degrades.

## 6 Real World Data

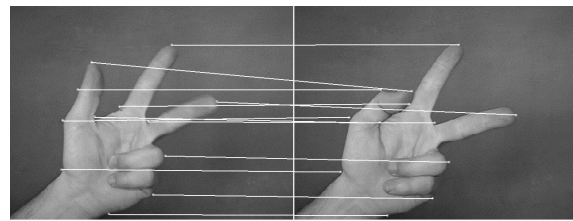
Our final piece of experimental work focusses on real-world data. Here we have matched images from a gesture sequence of a moving hand. The feature points in these images are points of maximum curvature on the outline of the hand. Figure 6.a shows the final configuration of correspondence matches obtained using our new method. For comparison Figure 6.b shows the correspondence matches obtained with SVD. In the case of the EM method, all the correspondence matches are correct, while in the case of SVD the two correspondences marked with circles are in error.

## 7 Conclusions

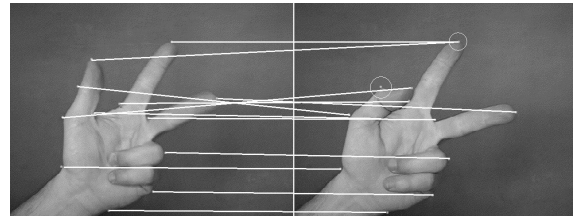
We have considered three ways of improving the recovery of point correspondences using spectral analysis of the point proximity matrix. The three lines of investigation are the use of an alternative proximity weighting matrix, the use of robust methods for comparing the eigenvectors of the proximity matrix, and, embedding the correspondence process within the EM algorithm. The first two refinements offer improved performance under point position error, but can not render the method robust to structural error (i.e. deletion or insertion of points). To overcome structural error, we embed the correspondence process within the EM algorithm.

## References

- [1] F.R.K. Chung, *Spectral Graph Theory*, CBMS series **92**, AMS Ed., 1997.
- [2] A.D.J. Cross, E.R. Hancock, "Graph matching with a dual step EM algorithm", *IEEE PAMI*, **20**, pp. 1236–1253, 1998.



(a) Final matches-EM



(b) Final matches-SVD

**Figure 3.**

- [3] A.P. Dempster, Laird N.M. and Rubin D.B., "Maximum-likelihood from incomplete data via the EM algorithm", *J. Royal Statistical Soc. Ser. B (method.)*, **39**, pp. 1-38, 1977.
- [4] K.Inoue and K. Urahama, "Sequential fuzzy cluster extraction by a graph spectral method", *Pattern Recognition Letters*, **20**, pp. 699-705, 1999.
- [5] M.I. Jordan and R.A. Jacobs, "Hierarchical mixtures of experts and the EM algorithm", *Neural Computation*, **6**, pp. 181-214, 1994.
- [6] G.L. Scott and H.C. Longuet-Higgins, "An algorithm for associating the features of 2 images", *Proceedings of the Royal Society of London Series B (Biol.)*, **244**, pp. 21–26, 1991.
- [7] K. Sengupta and K.L.Boyer, "Modelbase partitioning using property matrix spectra", *Computer Vision and Image Understanding*, **70**:2, pp. 177-196, 1998.
- [8] L.S. Shapiro and J.M. Brady, "Feature-based correspondence - an eigenvector approach", *Image and Vision Computing*, **10**, pp. 283–288, 1992.
- [9] J. Shi and J.Malik, "Normalized cuts and image segmentation", *Proc. of the IEEE Conf. on CVPR*, pp.731-737, 1997.
- [10] A. Shokoufandeh, S.J. Dickinson, K. Siddiqi and S.W. Zucker, "Indexing using a spectral encoding of topological structure", *Proc. of CVPR*, pp.491-497, 1999.
- [11] H. Sossa and R. Horaud, "Model indexing: the graph-hashing approach", *Proc. of the IEEE Conf. on CVPR*, pp. 811-815, 1992.
- [12] S. Umeyama, "An eigen-decomposition approach to weighted graph matching problems", *IEEE PAMI*, **10**, pp. 695–703, 1988.